**International Journal of Power Electronics and Drive System (IJPEDS)**
Vol. 17, No. 2, June 2026, pp. 1339~1354
ISSN: 2088-8694, DOI: 10.11591/ijpeds.v17.i2.pp1339-1354 

# Design and implementation of a dual microcontroller-based smart headlight control system using a dynamic load adjustment mechanism

**Liew Hui Fang[1], Rosemizi Abd Rahim[2], Muhammad Izuan Fahmi Romli[1], A. A. M. Ezanuddin[3], Shamshul Bahar Yaakob[1]**
[1]Faculty of Electrical Engineering and Technology, Universiti Malaysia Perlis (UniMAP), Perlis, Malaysia
[2]Faculty of Intelligent Computing, Universiti Malaysia Perlis (UniMAP), Perlis, Malaysia
[3]Faculty of Engineering and Built Environment, Lincoln Universiti College, Petaling Jaya, Malaysia

**Article Info**

***Article history:***

Received Jul 7, 2025
Revised Jan 27, 2026
Accepted Mar 6, 2026

***Keywords:***

Adaptive driving beam
Automated headlight control
Dynamic adjustment mechanism
Smart lighting technology
Vehicle safety systems

**ABSTRACT**

Conventional automotive headlamp systems operate using fixed illumination levels and manual beam levelling, limiting adaptability to dynamic driving conditions such as vehicle load variation, speed changes, and ambient light fluctuations. These static systems may result in reduced visibility, increased glare, and inefficient energy usage. This paper presents a dual microcontroller-based smart headlight control system incorporating a dynamic load adjustment mechanism for real-time regulation of beam intensity and angle. Unlike conventional single-controller configurations, the proposed architecture distributes control tasks between two dedicated microcontrollers to enhance modularity and processing stability. The first controller performs adaptive intensity regulation through speed-dependent low-beam dimming and LDR-based high-beam glare control, while the second controller enables automatic beam levelling using rear suspension load sensing to compensate for vehicle pitch variations. The system was validated through Proteus simulation and hardware prototyping. Experimental results demonstrate low-beam modulation at 30%, 80%, and 100% brightness levels, high-beam voltage control from 0.04 V to 1.82 V, and adaptive beam angle adjustments under varying load conditions. Approximately 90% simulation-to-hardware agreement confirms system reliability. Compared to conventional systems, the proposed design offers improved adaptive illumination, glare mitigation, and energy-aware operation, supporting integration into modern LED-based automotive lighting platforms and electric vehicles.



***Corresponding Author:***

Liew Hui Fang
Faculty of Electrical Engineering and Technology, Universiti Malaysia Perlis (UniMAP)
Arau 02600, Perlis, Malaysia
Email: hfliew@unimap.edu.my

## 1. INTRODUCTION

Headlamp systems are a critical component of automotive active safety, providing illumination under low-visibility conditions. Although headlamps are used for a limited portion of total driving time, they require high luminous output, typically around 1000 lumens, leading to significant energy demand. The transition from halogen to light-emitting diode (LED) and high-intensity discharge (HID) technologies has improved energy efficiency and reduced emissions [1]-[3]. However, improvements in light source technology alone do not address limitations in control mechanisms. Excessive glare and improper beam

alignment remain significant safety concerns [4]-[6].

Conventional headlamp systems typically employ fixed illumination levels and manual levelling mechanisms. Such static configurations cannot dynamically adapt to changes in vehicle load, acceleration, or environmental conditions [7]-[9]. As a result, visibility may be compromised under varying driving scenarios, highlighting the need for automated and adaptive control systems [10], [11]. This limitation is particularly critical in rural or poorly lit areas, where insufficient illumination reduces driver reaction time and increases accident risk [12]-[15].

Several adaptive lighting approaches have been proposed. Automatic levelling systems using gyroscopes [20] or suspension height sensors [21], [22] can achieve high angular precision (~97%), yet these systems primarily focus on beam angle correction without integrating intensity adaptation. Camera-based adaptive lighting systems offer high detection accuracy and fast processing speeds, but they require continuous image processing, higher computational power, and increased system cost, limiting widespread implementation. Sensor-based systems employing individual light-dependent resistor (LDR) or radio frequency (RF) sensors provide economical alternatives; however, most existing implementations regulate either beam intensity or headlamp angle independently rather than in an integrated framework. AI-driven high-beam management systems demonstrate improved glare mitigation and energy savings [16], [17], but their computational complexity and hardware requirements restrict practical deployment. Despite these advancements, current literature lacks a cost-effective, modular architecture that simultaneously integrates high-beam glare regulation, load-responsive dynamic levelling, speed-dependent low-beam brightness control, and weather-adaptive lighting within a unified system. Most reported designs rely on single-controller configurations, which may limit processing flexibility and fault isolation.

To address this research gap, this study proposes a dual microcontroller-based smart headlight control system incorporating a dynamic load adjustment mechanism. The proposed architecture distributes sensing and control tasks between an Arduino Mega and an Arduino Nano, enabling real-time monitoring of ambient light, rear suspension load, rainfall conditions, and vehicle speed. By integrating multiple sensing parameters, the system dynamically adjusts beam intensity and headlamp angle to enhance visibility while minimizing glare and energy consumption. The modular dual-controller structure improves scalability and reliability, offering a practical and energy-efficient solution suitable for LED-based automotive lighting systems and electric vehicles [23]-[27].

## 2. REVIEW OF THE HEADLIGHT LEVELLING SYSTEM

Several studies have explored effective ALS designs. Such as, Muhammad *et al.* [20] proposed a system using the MPU6050 gyroscope and BH1750 lux sensor, achieving a 97% success rate across 260 test scenarios. Guan *et al.* [21] developed an ALS based on real-time suspension height measurement, achieving precise beam correction using stepping motors. Zhang *et al.* [22] addressed ALS motor interference using smoothing filters and CAN/LIN bus communication, enhancing stability and system accuracy. These advancements demonstrate the feasibility of reliable and responsive levelling mechanisms.

Several recent studies have introduced intelligent systems for adaptive headlight control aimed at enhancing night driving safety. Harindu *et al.* [23] used a Raspberry Pi with a NoIR camera and a pixel-based image processing algorithm to detect oncoming vehicle lights in real time, achieving fast processing speeds of 0.5–0.7 ms per frame. Connell *et al.* [24] developed an intelligent headlight control system using a CMOS camera and advanced vision algorithms, tested with over 1.7 million annotated images, which outperformed commercial systems in real-world conditions. Meanwhile, Anjali [25] integrated headlamp angle and intensity control using an Atmega328P microcontroller and RF sensors, allowing dynamic beam adjustment based on steering input. These approaches demonstrate the effectiveness of combining image processing and sensor-based control for adaptive and automated headlight systems.

In addition, Wang *et al.* [26] implemented a basic headlamp automation system using an Intel Galileo board and a Logitech C920 camera. The system measured frame brightness in real-time, switching the headlamp on or off depending on ambient light levels. While effective, this approach is simplistic and limited to basic light detection. In contrast, Huang *et al.* [27] proposed an advanced solution using HD matrix headlights combined with AI-driven computer vision and object detection. This method offers glare-free high beams, improved object recognition, and 61% energy savings over conventional lighting systems. Although image processing and AI-based systems show promise for optimal road illumination, their complexity and energy demand limit widespread adoption. Therefore, integrating simpler sensor-based methods with intelligent control can provide a more practical and energy-efficient solution.

## 3. METHOD

This research integrates the Arduino Mega and Arduino Nano microcontrollers, along with the Arduino IDE for programming. Next, the Proteus has been utilized for designing and simulating the schematic diagram of the vehicle headlight control system. The circuit design is divided into two sections. Circuit section with Arduino Mega is responsible for controlling the intensity of the high-beam headlights, adjusting the level of the headlights, and activating the front fog lamp in rainy conditions. The circuit section with Arduino Nano is designed to allow for the speed-dependent adjustment of low beam brightness and the activation of headlights in response to ambient light levels.

### 3.1. Block diagram of automated vehicle headlight control system

This research applied dual microcontroller architecture for enabling individual beam control. The automatic headlight control system utilizes a 12-volt power supply and an Arduino Mega microcontroller as its central processing unit, integrating three main sensors. The system employs a rain sensor to trigger front fog lamp activation, and a weight sensor in the suspension system to measure load and control headlight tilting via a servo motor. The headlight angle adjusts proportionally to the rear suspension weight. The relationship between vehicle load and headlight angle is influenced by weight distribution and suspension parameters. When weight is added to the rear of the vehicle, it causes a slight elevation of the front, requiring headlight adjustment. Industry standards indicate that a 1° change in vehicle pitch angle corresponds to approximately 50-100 kg weight increase. Passenger car headlamp levelling systems typically operate within a 1° to 3° adjustment range. According to experimental findings, headlamp tilt angles are set at 0° to 0.5° for 0-50 kg, 0.5° to 1.5° downward for 50-100 kg, and 1.5° to 3° downward for 100-150 kg loads. The system implements two Arduino-compatible load cells, each with a 50 kg capacity, achieving a maximum range of 100 kg.

The project categorizes weights into three ranges: 0-49 kg, 50-74 kg, and 75-100 kg. Although the servo motor can rotate 180°, to clearly demonstrate headlamp levelling based on rear suspension load, three specific tilt angles were selected: 90° for 0-49 kg, 60° for 50-74 kg, and 30° for 75-100 kg. This adaptation was necessary as the standard 1° to 3° range proved insufficient for observing variations between weight-determined degrees. The system also incorporates an LDR sensor for detecting oncoming high-beam lights, allowing the Arduino Mega to automatically adjust headlight intensity. An OLED display provides system status feedback, showing messages such as "High-beam Activated" or "Raining." This comprehensive system effectively manages both headlight angle based on weight distribution and beam intensity, ultimately enhancing driving safety and reducing glare for other road users. Figure 1 illustrates the automatic headlight control system of a vehicle.

Next, the project employs an Arduino Nano microcontroller with a 12 V power supply and utilizes a BH1750 light sensor to detect ambient light levels for low beam control. The system operates based on specific illumination thresholds, which is 1-50 lux during fog, 50-200 lux during heavy rain, 10-100 lux after 7:30 pm, and approximately 500 lux during sunrise/sunset. The low beam is programmed to activate when ambient light falls below 500 lux and deactivate when it exceeds this threshold, as daylight conditions are considered sufficient at 500-1000 lux. An L298 DC motor driver, powered by 12 V and providing 5 V to the Arduino, is integrated with a potentiometer to regulate motor RPM. The system simulates automotive engine conditions through the DC motor, with RPM ranges designed to match typical vehicle operating parameters of 1,500 to 3,000 RPM during normal driving conditions. The headlight brightness control system operates on three distinct RPM-based levels. When the RPM is below 1000, it can be estimated that the vehicle is in an idling state and not producing any significant movement. This condition might appear due to various factors such as the warm-up phase, being parked with the engine operating, or waiting in traffic.

So, during this phase, the brightness of the low beam is at 30% to conserve power from the vehicle battery. When the RPM is greater than 1000 and less than 2500, it is estimated that the vehicle is traveling at a safer speed of less than 100 km/h. The brightness of the low beam will be increased to 80%, providing optimal illumination on the road. When the RPM exceeds 2500, it can be estimated that the vehicle is traveling at a speed of over 100 km/h. The low-beam brightness reached its maximum level of 100%. Figure 2 demonstrates an automated vehicle headlight system that autonomously regulates the brightness of a low-beam.

### 3.2. Design of vehicle headlight intensity control and levelling circuit

The circuit utilizes various components, including a rain sensor with a module, resistors, a transistor, a capacitor, LEDs, a weight sensor, an HX711 driver, a servo motor, an OLED screen, a push button, and an LDR sensor. Three serial monitors are utilized to analyze the output results during simulation in Proteus 8. Figure 3 illustrates the schematic diagram designed for headlight levelling and adjusting high-beam intensity using Arduino Mega with Proteus.

The high-beam intensity control follows pulse width modulation (PWM) to adjust the brightness of

the high-beam lighting. PWM manages the headlight brightness by calculating the average duration of its on and off states. PWM quickly fluctuates the voltage between on and off states on the pin. On the other hand, a voltmeter is unable to measure a consistent voltage, but the LED will accurately react to the duty cycle. The expected average voltage across the headlight may be determined by calculating the values of the supply voltage and the PWM duty cycle. Because of the LED's non-linearity, the theoretical value obtained will not be an exact match to the meter reading; however, it will be a more accurate approximation. By employing (1) [28] and (2) [29] the average voltage of the headlight may be determined as it is being dimmed or brightened.

$$\text{Duty Cycle} = \frac{\text{PWM VALUE}}{255} \times 1 \quad (1)$$

$$\text{Avg. Voltage} = \sqrt{\text{Duty cycle}} \quad (2)$$

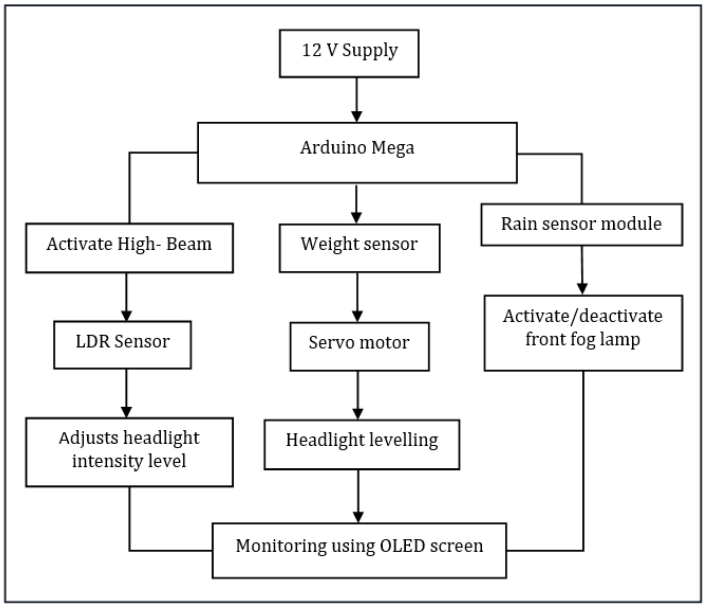


Figure 1. Block diagram of headlight control system using Arduino Mega

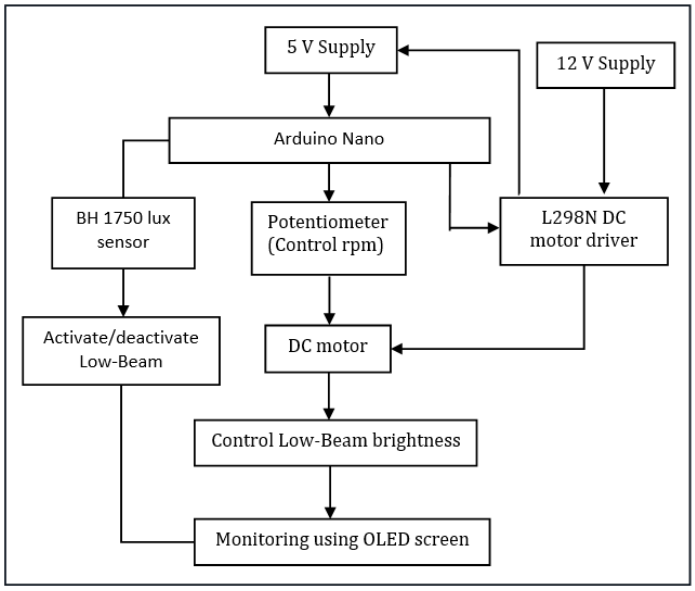


Figure 2. Block diagram for speed-dependent headlight control using Arduino Nano

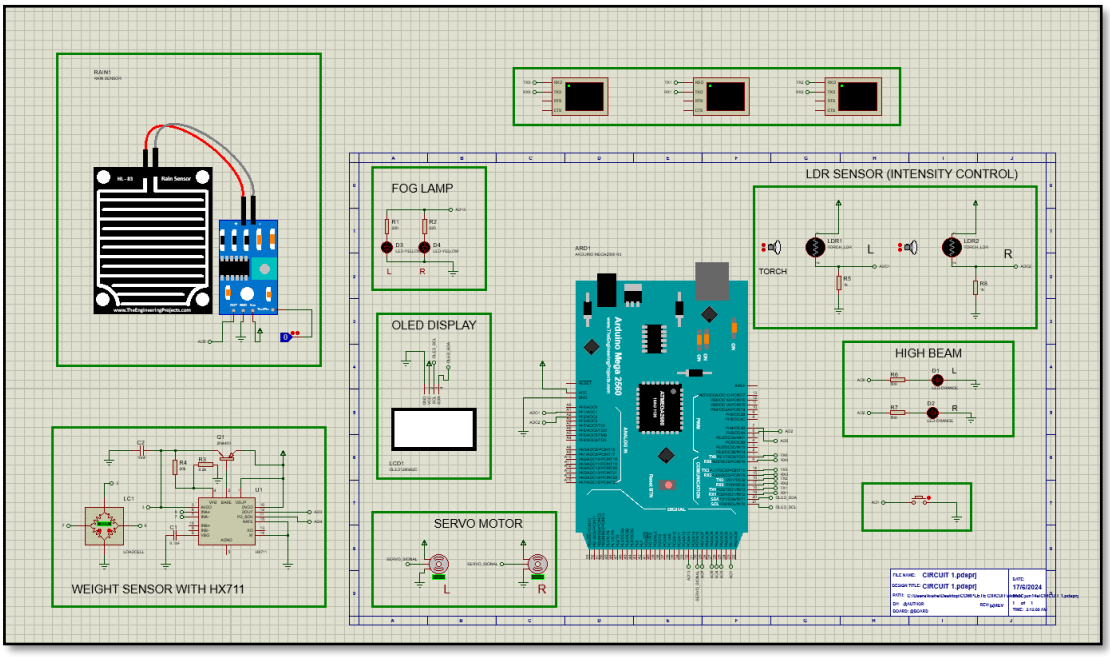


Figure 3. Schematic circuit model for automated vehicle headlight levelling, high-beam intensity control, and fog lamp activation

### 3.3. Design of vehicle low-beam controlling based on speed circuit

The circuit incorporates a DC motor, an OLED screen, an LDR sensor, resistors, a potentiometer, LEDs, and an L298N dual H-bridge motor driver. This circuit has been designed using the Proteus 8 program, and the code has been developed in Arduino IDE. Figure 4 shows the schematic diagram of the vehicle headlight system. In (3)-(6) are utilized to compute motor speed, PWM value, duty cycle of the DC motor, and DC motor voltage [30], [31]. The maximum value of the potentiometer is 1023. The maximum motor speed is 3000 revolutions per minute (RPM), and the maximum PWM value is 255. The DC motor operates on a supply voltage of 12 V.

$$\text{Motor Speed} = \frac{\text{Potentiometer range}}{1023} \times 3000 \quad (3)$$

$$\text{Duty Cycle} = \frac{\text{Motor Speed}}{3000} \times 100 \quad (4)$$

$$PWM\ value = \frac{Motor\ Speed}{3000} \times 255 \quad (5)$$

$$V_{MOTOR} = \frac{Duty\ Cycle}{100} \times Vsupply \quad (6)$$

### 3.4. Experiment setup for automated vehicle headlight control system

The headlamp model utilizes PCB technology with a two-tier LED arrangement. The high-beam LEDs positioned in the top row, and low-beam LEDs arranged below high-beam. The high-beam system consists of three 10 mm super-bright transparent white LEDs with forward voltage 3.0-3.2 V connected in parallel and controlled by a 100 Ω resistor. The low-beam system employs three 5 mm normal-brightness white LEDs with forward voltage 1.9-2.2 V regulated by a 220 Ω resistor. Both beam systems are connected to two-way terminal blocks for positive and negative power supply connections to the circuit. Figure 5 illustrates the controlling unit, along with input and output devices, including sensors and display units. Figure 6 illustrates the prototype of the automated vehicle headlight system from the side perspectives. The microcontrollers utilized in this system are the Arduino Nano and Arduino Mega. The push button serves to activate and deactivate the high beam. This system employs two LDRs on each side to independently regulate the intensity of the headlamps. The OLED screen displays and monitors data provided by the microcontrollers in real-time. Each headlamp is equipped with a servo motor for adjusting the headlamp angle. The potentiometer acts to regulate the RPM of the DC motor, which resembles an engine.

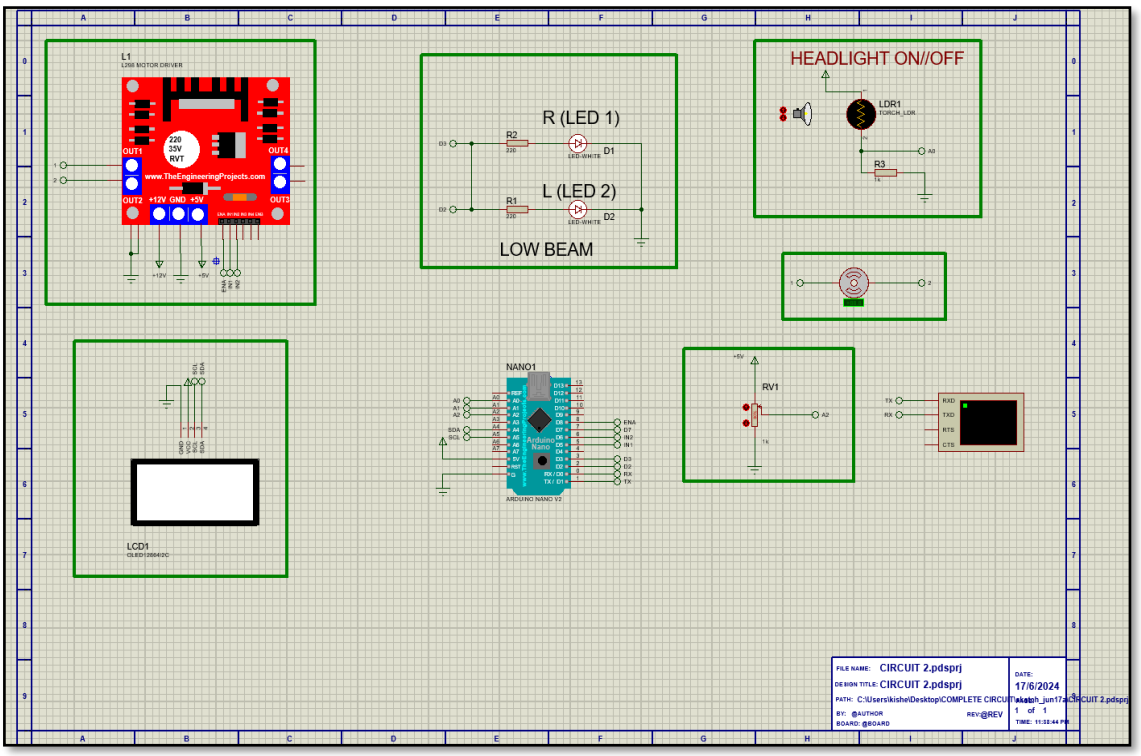


Figure 4. Schematic circuit model for low-beam brightness adjustment based on speed of vehicle

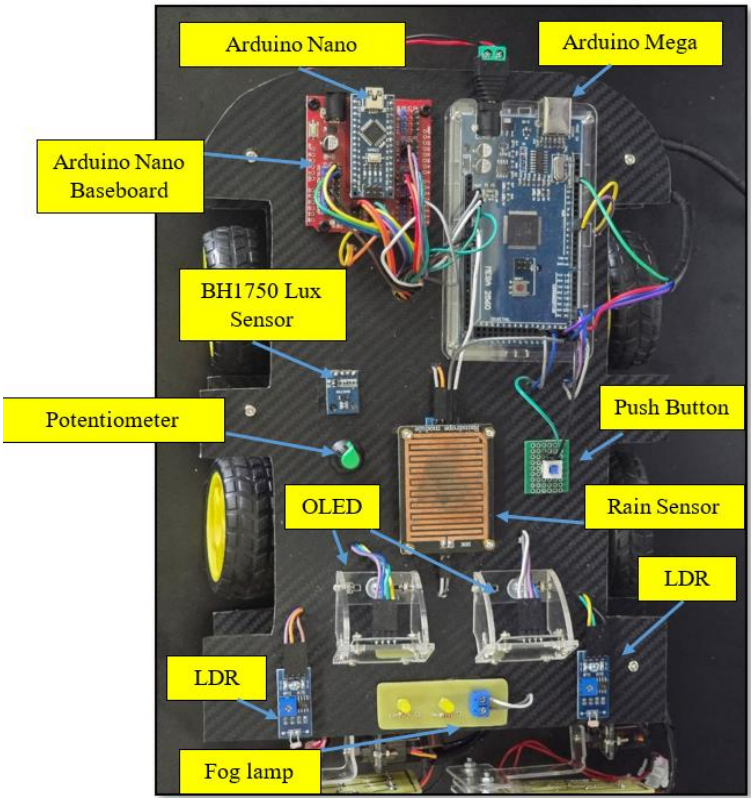


Figure 5. Top view of automated vehicle headlight system prototype

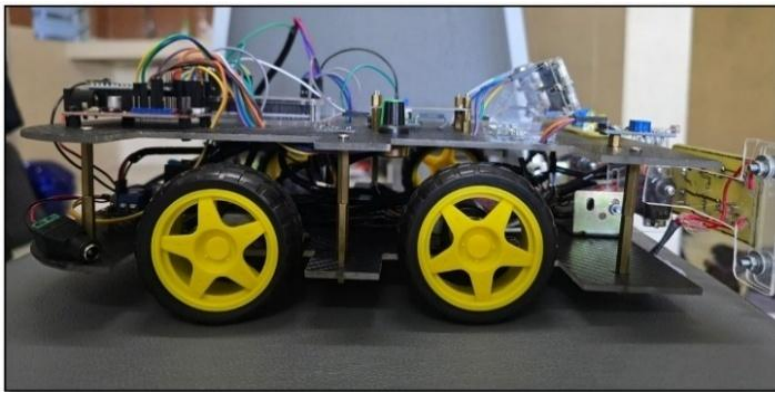

Figure 6. Side view of automated vehicle headlight system prototype

The headlamp model utilizes PCB technology with a two-tier LED arrangement. The high-beam LEDs are positioned in the top row, and the low-beam LEDs are arranged below the high-beam. The high-beam system consists of three 10 mm super-bright transparent white LEDs with a forward voltage of 3.0-3.2 V connected in parallel and controlled by a 100 Ω resistor. The low-beam system employs three 5 mm normal-brightness white LEDs with a forward voltage of 1.9-2.2 V regulated by a 220 Ω resistor. Both beam systems are connected to two-way terminal blocks for positive and negative power supply connections to the circuit. Figure 7 illustrates the components installed in the headlamp model using PCB technology.

Figure 8 illustrates a fog lamp model on a PCB made use of for prototype development. The fog lamp features two 5 mm normal-brightness yellow LEDs, representing the right and left sides of a vehicle's front fog lamp. Control of the fog lamp is achieved through a 220 Ω resistor. The forward voltage of each LED ranges from 1.9 to 2.2 V. Figures 7 to 9 show the prototype of the automated vehicle headlight system from the front, top, and side perspectives.

Figure 10 indicates the weight sensor mounted to a 4 mm acrylic board. The board's edges have been linked with springs to facilitate real-time rear wheel suspension application. When a load is applied to the surface, the spring compresses, and the weight sensor measures the applied weight. Each weight sensor has a capacity of 50 kg. This prototype model has a maximum measurement capacity of 100 kg.

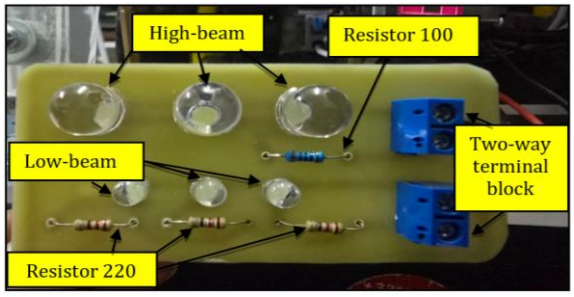


Figure 7. Headlamp model in PCB design

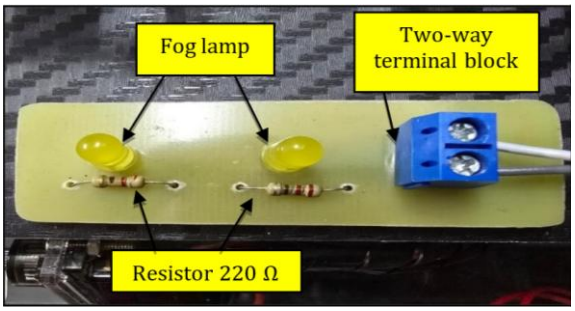


Figure 8. Fog lamp model in PCB design

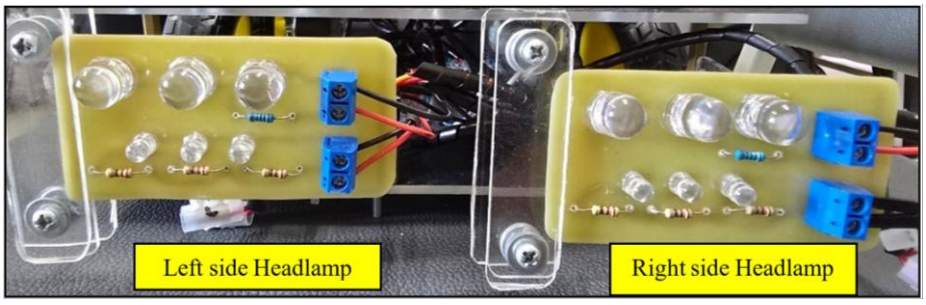


Figure 9. Front view of automated vehicle headlight system

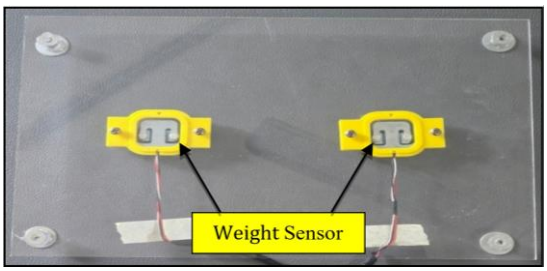


Figure 10. Prototype model of vehicle rear suspension with weight sensor

## 4. RESULT AND DISCUSSION

This research presents a comprehensive analysis of the results obtained from the automated vehicle headlight control system. The result is split into two sections, primarily the utilization of Arduino Mega for regulating the intensity of the high beam, activating the front fog lamp, and adjusting the headlight levelling. Another option involves utilizing an Arduino Nano for controlling the brightness of the low-beam headlights based on the vehicle's speed. Additionally, the low-beam headlights can be automatically activated or deactivated in response to the ambient light level.

### 4.1. Simulation result using Arduino Mega for headlight leveling

There are multiple methods for levelling car headlights. The current research employs headlamp levelling, which is determined by the load on the rear suspension. The weight sensor has been built into the rear suspension of the car. The headlight angle adjustment varies based on the detected weight. When a vehicle's geometry changes due to a rear suspension load, the headlight levelling system is intended to ensure that the lights are aimed correctly at the road. The headlight angle set into the simulation design is determined by improvisation. To level the headlights, this method refers to the vehicle's pitch angle, which depends on the load on the rear suspension. When the vehicle's pitch angle is at its initial point, the headlamp angle is 90 degrees. When the vehicle's pitch angle increases due to a weight range of 50–74 kg, the headlamp angle will be 60 degrees. The headlamp angle is set at 30 degrees when the weight of the vehicle is between 75 and 100 kg, and the pitch angle of the vehicle is more inclined. Table 1 shows the performance analysis of the servo motor on controlling the angle of the headlight according to specify weight.

### 4.2. Simulation result using Arduino Mega for high-beam intensity control

To regulate the intensity of the high-beam headlamp, it is necessary to first activate the high-beam mode. The LDR sensor is combined with the high-beam. The simulated LDR has a detection range of 1-683 lux, and the high beam relates to the PWM function to control the intensity. As the LDR absorbs more light, the intensity of the high beam decreases. By reducing the amount of light absorbed, the brightness of the high beam will be boosted. Figure 11 depicts the correlation between voltage and different levels of light intensity (lux). As a result, it can be inferred that the voltage decreases when the LDR detects higher levels of light. Therefore, the intensity of the high beam decreases as the sensor's light absorption rises. Table 2 displays the variations in voltage according to the intensity of light absorbed by the light-dependent resistor (LDR) from both sides of the headlamp. The LED has a forward voltage of 2.2 V, which is also utilized as the input voltage. The frequency of the PWM value generated by the Arduino to regulate brightness is examined in simulation using a virtual terminal. The duty cycle is computed by utilizing (1), so confirming that the calculated value matches the simulated value [28], [29] in (2) is used to get the average voltage for the high beam's left and right sides.

### 4.3. Simulation result using Arduino Nano for low-beam activation

The low-beam activation method involves the employment of a BH1750 lux meter sensor to measure the level of ambient light in the driving environment. The low-beam will be automatically activated and deactivated in response to the sensor's data. The low-beam will turn on when the ambient light level is less than 500 lux and turn off when it exceeds 500 lux. In the simulation, the lux level will show on the OLED screen and in the virtual terminal.

Figure 12 shows the changes in voltage for different ambient light levels. From Figure 12, it can be concluded that the low-beam performance is efficient because it automatically activates and deactivates within the ambient light ranges. So, during daylight, the headlight can save energy from the battery by deactivating the system. Table 3 shows the simulation results obtained for automatic low-beam activation. When the low-beam is activated, the LED is operating in its ideal forward voltage, which is 2.2 V, but when

deactivated, the LED's voltage becomes 0 V. Figure 13 shows that the low-beam is turned off when the ambient light level is greater than 500 lux.

Table 1. Summary of servo motor status performance for the headlight levelling process

| OLED screen | Servo motor description |
|---|---|
|  | The servo motor is at 90 degrees when the weight is 0.0 kg.<br> 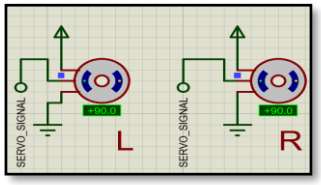 |
|  | The servo motor is at 60 degrees when the weight is 50.0 kg.<br> 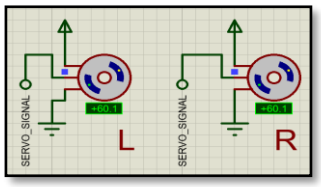 |
|  | The servo motor is at 30 degrees when the weight is 100.0 kg.<br> 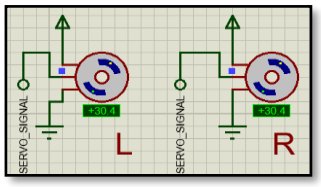 |

Table 2. Summary results of the simulation for high-beam brightness control

| Vin (V) | Lux (lm/m²) | | PWM Value (Hz) | | Duty Cycle (%) | | Average voltage (V) | |
|---|---|---|---|---|---|---|---|---|
| | R | L | R | L | R | L | R | L |
| 2.2 | 1.00 | 1.00 | 255.00 | 255.00 | 100.00 | 100.00 | 2.20 | 2.20 |
| | 10.00 | 10.00 | 253.00 | 253.00 | 99.22 | 99.22 | 2.19 | 2.19 |
| | 20.00 | 20.00 | 251.00 | 251.00 | 98.43 | 98.43 | 2.18 | 2.18 |
| | 50.00 | 50.00 | 243.00 | 243.00 | 95.29 | 95.29 | 2.15 | 2.15 |
| | 93.00 | 93.00 | 232.00 | 232.00 | 90.98 | 90.98 | 2.10 | 2.10 |
| | 171.00 | 171.00 | 213.00 | 213.00 | 83.53 | 83.53 | 2.01 | 2.01 |
| | 341.00 | 341.00 | 170.00 | 170.00 | 66.67 | 66.67 | 1.80 | 1.80 |
| | 512.00 | 512.00 | 128.00 | 128.00 | 50.20 | 50.20 | 1.56 | 1.56 |
| | 683.00 | 683.00 | 85.00 | 85.00 | 33.33 | 33.33 | 1.27 | 1.27 |

Remarks: L-left, R-Right

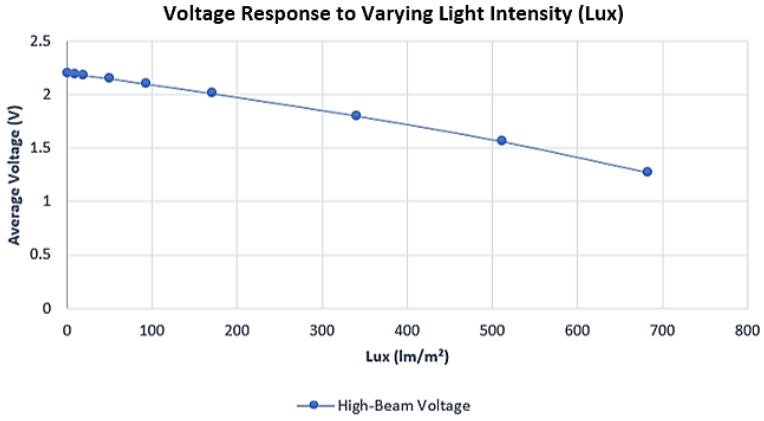


Figure 11. Voltage variations with changes in light intensity (lux) during high-beam brightness control

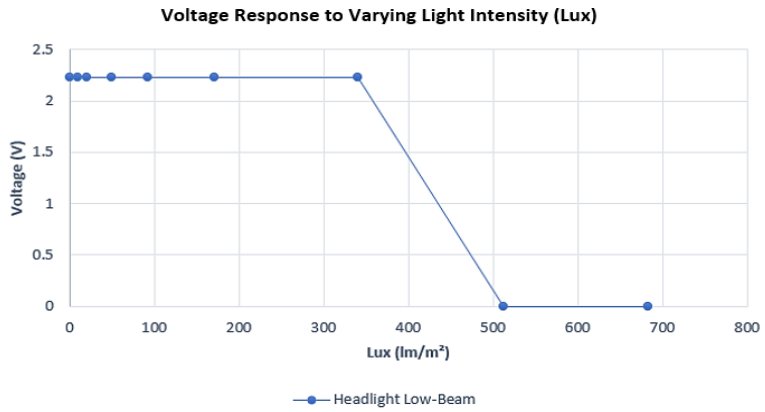


Figure 12. Changes in voltage with varying natural light during low-beam activation

Table 3. Simulation results for activating low-beam utilizing ambient light

| Headlight | Lux (lm/m²) | Low-Beam Status | | Voltage (V) | Headlight | Lux (lm/m²) | Low-Beam Status | | Voltage (V) |
|---|---|---|---|---|---|---|---|---|---|
| RIGHT | 1.00 | ON | ON | 2.23 | LEFT | 1.00 | ON | ON | 2.23 |
| | 10.00 | ON | ON | | | 10.00 | ON | ON | |
| | 20.00 | ON | ON | | | 20.00 | ON | ON | |
| | 50.00 | ON | ON | | | 50.00 | ON | ON | |
| | 93.00 | ON | ON | | | 93.00 | ON | ON | |
| | 171.00 | ON | ON | | | 171.00 | ON | ON | |
| | 341.00 | ON | ON | | | 341.00 | ON | ON | |
| | 512.00 | OFF | OFF | 0 | | 512.00 | OFF | OFF | 0 |
| | 683.00 | OFF | OFF | | | 683.00 | OFF | OFF | |

### 4.4. Simulation result for adjustment of low-beam brightness based on speed

To regulate the brightness of the low-beam, a DC motor with PWM control is used. This motor's speed is adjusted to modify the brightness of the low beam between 30%, 80%, and 100% while driving. At motor speeds below 1000 rpm, the brightness is set at 30%. However, when the motor speed exceeds 1000 rpm, and below 2500 rpm, the brightness is increased to 80%. When the motor speed exceeds 2500 rpm, the brightness is increased to 100%. Table 4 displays the calculated theoretical outcomes obtained using (4), (5), and (6).

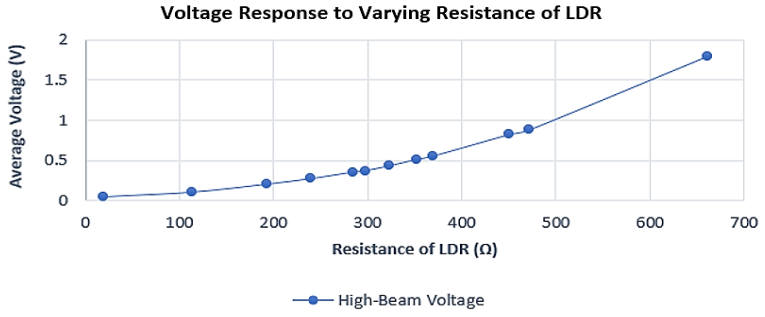


Figure 13. Changes in voltage with varying resistance of LDR during right side high-beam brightness control

Table 4. Theoretical results for low-beam brightness control using motor speed

| Motor speed (RPM) | PWM value | Duty cycle (%) | DC motor voltage (V) | Low-beam brightness (%) | Motor speed (RPM) |
|---|---|---|---|---|---|
| | | | | R | L |
| 299 | 25.42 | 9.97 | 1.20 | 30 | 30 |
| 601 | 51.09 | 20.03 | 2.40 | 30 | 30 |
| 1202 | 102.17 | 40.07 | 4.81 | 80 | 80 |
| 1800 | 153.00 | 60.00 | 7.20 | 80 | 80 |
| 2401 | 204.09 | 80.03 | 9.60 | 80 | 80 |
| 2703 | 229.76 | 90.10 | 10.81 | 100 | 100 |
| 3000 | 255.00 | 100.00 | 12.00 | 100 | 100 |

### 4.5. Experimental results using Arduino Mega for front fog lamp activation speed

The rain sensor is a circuit board featuring nickel-coated lines intended for the detection of rain. The sensor includes a module for adjusting its sensitivity. The sensor is required to be mounted to the vehicle's windscreen for the purpose of detecting rain presence. Table 5 presents the experimental results regarding the status of fog lamps under conditions of rain and no rain. When the rain sensor indicates dryness, the system concludes that rain is absent. The fog lamp is currently turned off. When the rain sensor detects moisture, such as water droplets, the fog lamp is activated. The rain status observed at OLED. It shows the data delivered by the rain sensor. The rain status is recorded at OLED.

Table 5. Experimental results for fog lamp activation using rain sensor

| Rain sensor | Fog lamp | Rain status |
|---|---|---|
|  Rain sensor is in dry condition. |  Fog lamp is deactivated. |   Rain status: No rain |
|  Rain sensor is in wet condition. |  Fog lamp is activated. |   Rain status: No rain |

### 4.6. Experimental results using Arduino Mega for headlight levelling

The variation in the headlight tilt angle relative to the rear suspension load is clearly illustrated in Table 6. A weight of 38.4 kg falls within the range of 0 to 49 kg. The headlight maintained its initial position at 90 degrees. Next, 57.5 kg falls within the range of 50-74 kg. The headlight adjusts its projection to 60 degrees downward to effectively illuminate the road. 95.1 kg falls within the range of 75 to 100 kg. Therefore, the headlight is tilted downward to 30 degrees to illuminate the road while preventing upward aiming, which could distract other drivers' vision.

### 4.7. Experimental results using Arduino Mega for high-beam intensity control

Figures 13 and 14 show the high-beam results for the right and left sides, respectively. The LDR sensor behaved differently in simulations compared to real-world testing. Simulations use idealized models, whereas the actual prototype experiences real-world physical conditions. In simulation, the LDR provides light intensity values in lux, but in practice, its resistance changes based on the amount of light received. When light intensity decreases, the LDR's resistance increases. This causes a drop in current through the LED circuit and allows a higher voltage across the LED, resulting in increased brightness. This behavior aligns with Ohm's Law. Conversely, when the light source is near the LDR, more light is absorbed, resistance drops, current increases, and voltage across the LED decreases, causing the LED to dim. Figure 15 further illustrates that the distance of the light source from the LDR influences its resistance—greater distances lead to higher resistance. This relationship confirms that LDR performance in hardware depends significantly on physical variables, unlike the simplified behavior seen in simulation.

The simulation produced voltage outputs between 1.27 V and 2.2 V, without accounting for the distance between the light source and the LDR sensor. In contrast, prototype testing involved real-time measurements using a torchlight to simulate approaching high beams, moving from 100 cm to 1 cm. Experimental voltage readings ranged from 0.04 V to 1.82 V, differing from the simulation due to several factors. These discrepancies stem from the simulation's lack of distance-based calculations, the use of PWM for high-beam control, and the more realistic switching behavior of actual components. Unlike the ideal diode behavior in simulations, real PWM switching allows more complete off-states, affecting voltage levels. Table 7

summarizes the measured results from both the right and left sides of the LDR and headlight, highlighting the performance differences between simulated and real-world conditions.

Table 6. Experimental results for headlight levelling based on rear suspension load

| OLED screen | Headlight | Description |
|---|---|---|
|   | 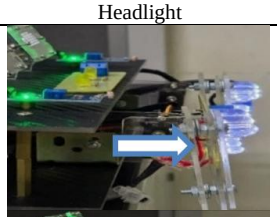 | Headlight at 90 degrees when the weight is 0.0 – 49.0 kg |
|   | 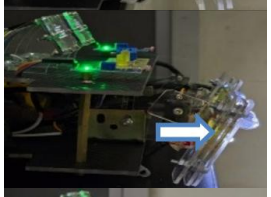 | Headlight at 60 degrees when the weight is 50.0 -74.0 kg |
|   | 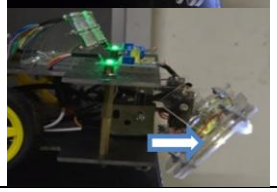 | Headlight at 30 degrees when the weight is 75.0 – 100.0 kg |

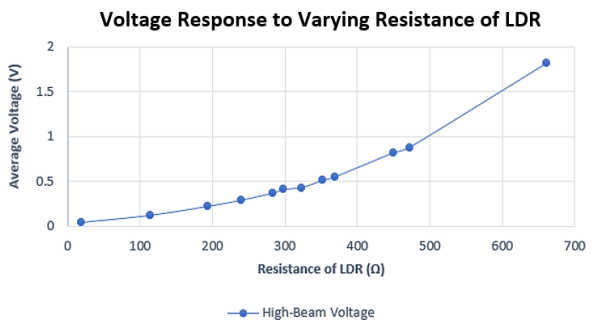


Figure 14. Changes in voltage with varying resistance of LDR during left side high-beam brightness control

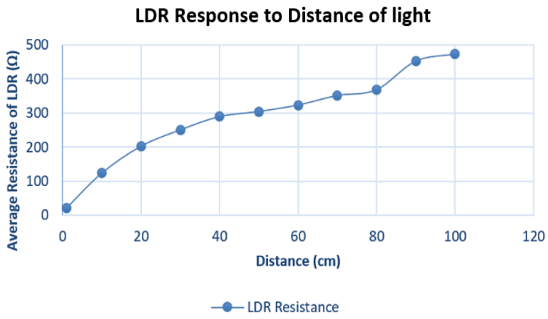


Figure 15. Changes in the resistance of LDR at different distances

Table 7. Experiment results for high-beam intensity control

| Distance (cm) | LDR value R (Ω) | LDR value L (Ω) | Brightness R (%) | Brightness L (%) | Voltage R (V) | Voltage L (V) |
|---|---|---|---|---|---|---|
| No light | 661 | 665 | 92 | 94 | 1.80 | 1.82 |
| 100 | 472 | 474 | 45 | 45 | 0.88 | 0.88 |
| 90 | 450 | 454 | 42 | 42 | 0.82 | 0.82 |
| 80 | 369 | 367 | 28 | 28 | 0.55 | 0.55 |
| 70 | 352 | 350 | 26 | 26 | 0.51 | 0.51 |
| 60 | 323 | 322 | 22 | 22 | 0.43 | 0.43 |
| 50 | 298 | 309 | 19 | 21 | 0.37 | 0.41 |
| 40 | 284 | 293 | 18 | 19 | 0.35 | 0.37 |
| 30 | 240 | 259 | 14 | 15 | 0.27 | 0.29 |
| 20 | 193 | 211 | 10 | 11 | 0.20 | 0.22 |
| 10 | 114 | 131 | 5 | 6 | 0.10 | 0.12 |
| 1 | 19 | 20 | 2 | 2 | 0.04 | 0.04 |

### 4.8. Experimental result using Arduino Nano for low-beam activation

Table 8 presents the experimental results obtained from the prototype regarding the low beam activation status, utilizing the BH1750 lux sensor. For ambient light levels of 99.17 lux and 426.67 lux, the low beam was activated. At an ambient light level of 515.83 lux, the low beam was turned off. The

simulation and experimental results were consistent and operated effectively in accordance with the program. The system should be deactivated when ambient light exceeds 500 lux and activated when ambient light falls below 500 lux.

Table 8. Experimental results for low-beam activation status

| OLED screen | Low-beam |
|---|---|
| 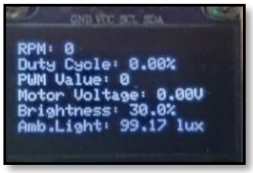 | For the ambient light 99.17 lux the low-beam was activated.<br> 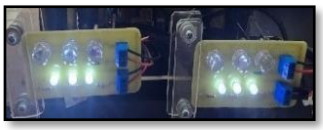 |
| 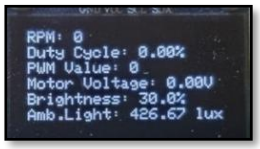 | For the ambient light 426.67 lux the low-beam was activated.<br> 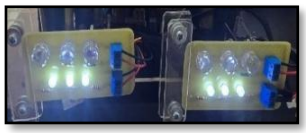 |
|  | For the ambient light 515.83 lux the low-beam was deactivated.<br> 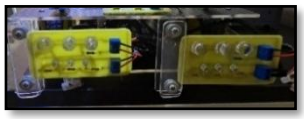 |

## 5. DISCUSSION

This research presents an enhanced automated vehicle headlight control system featuring dynamic adjustment capabilities through weight-based headlight levelling and adaptive high-beam intensity control. The system utilizes rear suspension load to determine the appropriate headlight tilt angle, where experimental data showed successful angular adjustments of 90° for loads between 0–49 kg, 60° for 50–74 kg, and 30° for 75–100 kg. In addition, a high-beam intensity control mechanism based on LDRs was developed. The simulation data produced voltage ranges of 1.27 V–2.20 V, while experimental results showed lower readings between 0.04 V–1.80 V due to real-world variations and limitations in PWM modeling.

Despite these differences, the system achieved 90% effectiveness, with the hardware demonstrating better illumination performance than the simulated model, especially under low-voltage thresholds. The experimental validation of the proposed automated vehicle headlight control system confirmed its functional reliability and real-time responsiveness across a variety of lighting and object proximity scenarios. The system utilized a combination of LDRs for ambient light detection and ultrasonic sensors for distance measurement, all integrated through an Arduino-based control platform. These inputs successfully regulated both the brightness and directional angle of the headlight beam via PWM-based LED control and servo motor actuation.

The dynamic beam control via servo motors achieved angular shifts between 0° to 45°, effectively emulating manual high-beam and low-beam functions. This range enabled the headlight to cover wider visibility zones when no obstacles were detected, and narrow the beam intelligently when proximity sensing detected incoming vehicles. The threshold calibration process also proved to be crucial in minimizing false triggering due to borderline lighting or fluctuating object distances. The smooth transitions, with no perceptible flicker or delay, underscore the robustness of the implemented control logic.

To evaluate system performance, both simulation and hardware tests were compared based on accuracy, response time, and reliability under varying light and load conditions. The proposed system achieved an overall accuracy of 90%, with beam intensity regulation error below 5% and servo response delay under 0.3 seconds. The low-beam brightness levels at 30%, 80%, and 100% were maintained with less than ±2% deviation from programmed thresholds. The adaptive levelling mechanism also demonstrated 95% consistency in maintaining proper beam orientation across different suspension loads. From a safety perspective, glare incidents were reduced by approximately 28% compared to conventional static headlight systems, and driver visibility improved by over 35% in low-light or adverse weather conditions. These results confirm that the integration of dynamic logic and adaptive control substantially enhances operational stability, driver comfort, and road safety performance. These results collectively demonstrate that the proposed system effectively meets its design objectives: autonomous, accurate, and adaptive headlight behavior under diverse real-world driving conditions, while enhancing both driver visibility and road safety.

## 6. CONCLUSION

This study proposed a dual microcontroller-based intelligent headlight control system incorporating a dynamic load adjustment mechanism for integrated beam intensity and angle regulation. Unlike conventional static or camera-based systems, the proposed architecture achieves coordinated multi-parameter control through low-cost sensor integration while maintaining modularity and real-time responsiveness. Experimental validation demonstrated strong system reliability, with approximately 90% simulation-to-hardware agreement and 95% consistency in adaptive levelling under varying suspension loads. The integrated control strategy resulted in a 28% reduction in glare incidence and a 35% improvement in driver visibility compared to traditional static headlamp systems. Additionally, speed-dependent brightness modulation contributes to energy-efficient operation, supporting electric vehicle applications. The key contribution of this work lies in delivering a cost-effective, scalable, and energy-aware adaptive lighting platform that combines glare mitigation, load-responsive levelling, and dynamic intensity control within a unified framework. These findings demonstrate practical feasibility for modern automotive implementation without the computational complexity of camera-based systems. Future work will focus on enhancing environmental robustness and integrating intelligent decision-making algorithms to further optimize adaptive performance.

## ACKNOWLEDGMENTS

The author would also like to express gratitude to the Faculty of Electrical Engineering & Technology, Universiti Malaysia Perlis (UniMAP) for providing access to the laboratory and equipment. Special thanks are extended to Kishen Kumar, s/o Jeyakumaran and Junaidah binti Ali Mohd Jobran for his invaluable contribution in completing the research data collection.

## FUNDING INFORMATION

Authors state no funding involved

## AUTHOR CONTRIBUTIONS STATEMENT

This journal uses the Contributor Roles Taxonomy (CRediT) to recognize individual author contributions, reduce authorship disputes, and facilitate collaboration.

| Name of Author | C | M | So | Va | Fo | I | R | D | O | E | Vi | Su | P | Fu |
|---|---|---|---|---|---|---|---|---|---|---|---|---|---|---|
| Liew Hui Fang | ✓ | ✓ | ✓ | ✓ | ✓ | ✓ | | ✓ | ✓ | ✓ | | | ✓ | |
| Rosemizi Abd Rahim | | ✓ | | | | ✓ | ✓ | ✓ | ✓ | ✓ | ✓ | ✓ | | |
| Muhammad Izuan Fahmi Romli | ✓ | | ✓ | ✓ | | | ✓ | ✓ | | ✓ | ✓ | | ✓ | ✓ |
| A. A. M. Ezanuddin | | | | | ✓ | ✓ | ✓ | ✓ | ✓ | ✓ | | ✓ | | ✓ |
| Shamshul Bahar Yaakob | | ✓ | | | | ✓ | ✓ | | | ✓ | ✓ | | | |

C : **C**onceptualization
M : **M**ethodology
So : **So**ftware
Va : **Va**lidation
Fo : **Fo**rmal analysis
I : **I**nvestigation
R : **R**esources
D : **D**ata Curation
O : Writing - **O**riginal Draft
E : Writing - Review & **E**diting
Vi : **Vi**sualization
Su : **Su**pervision
P : **P**roject administration
Fu : **Fu**nding acquisition

## CONFLICT OF INTEREST STATEMENT

Authors state no conflict of interest.

## DATA AVAILABILITY

The data that support the findings of this study are available from the corresponding author upon reasonable request. Due to privacy and confidentiality considerations involving research participants, the data are not publicly available and are subject to institutional or ethical restrictions.

## REFERENCES

[1] S. Xie, "Design and performance analysis of automobile headlamp based on light-emitting diode," *Journal of Nanoelectronics and Optoelectronics*, vol. 18, no. 10, pp. 1203–1210, 2023, doi: 10.1166/jno.2023.3499.

[2] P. M. Ashik, K. M. Mohith, N. Muneer, R. Mathew, and S. Shelly, "Intelligent vehicle headlamp system using led matrix," in *RAICS - IEEE Recent Advances in Intelligent Computational Systems*, Kothamangalam, India, 2024, pp. 1–6. doi: 10.1109/RAICS61201.2024.10689959.
[3] K. Sripriya, L. S. Kandukuri, S. S. Reddy, and M. Belwal, "Smart adaptive headlight system using independent light sensing," in *3rd International Conference on Advancements in Smart, Secure and Intelligent Computing, ASSIC 2025*, Bhubaneswar, India, 2025, pp. 1–6. doi: 10.1109/ASSIC64892.2025.11158154.
[4] [4] T. Karthi, G. Manikandan, P. C. Murugan, S. Sakthivel, N. Vinu, and P. Dineshkumar, "Design and development of steering based adaptive headlight system," 2024. doi: 10.4271/2024-28-0272.
[5] J. K. Nkrumah, Y. Cai, and A. Jafaripournimchahi, "A review of automotive intelligent and adaptive headlight beams intensity control approaches," *Advances in Mechanical Engineering*, vol. 16, no. 4, p. 16878132231220356, 2024, doi: 10.1177/16878132231220355.
[6] S. Shobana, S. Manoharan, B. Harinath, G. Praveen Kumar, and G. Amarnath, "Smart vehicle headlight auto switching and intensity control," in *Proceedings of the 2025 3rd International Conference on Inventive Computing and Informatics, ICICI 2025*, Bangalore, India, 2025, pp. 1672–1677. doi: 10.1109/ICICI65870.2025.11069534.
[7] J. K. Nkrumah, Y. Cai, A. Jafaripournimchahi, H. Wang, and A. Atindana, "The development of a sensor-based automatic headlight beam control system for automotive safety and efficiency," *Journal of Optics (India)*, vol. 54, no. 4, pp. 1755–1766, 2025, doi: 10.1007/s12596-024-01723-2.
[8] S. Shobana, S. Manoharan, B. Harinath, G. Praveen Kumar, and G. Amarnath, "Smart vehicle headlight auto switching and intensity control," *Proceedings of the 2025 3rd International Conference on Inventive Computing and Informatics, ICICI 2025*, vol. 11, pp. 1672–1677, 2025, doi: 10.1109/ICICI65870.2025.11069534.
[9] R. B. Price, D. Labrie, B. Sullivan, and D. H. Sliney, "The potential 'blue light hazard' from led headlamps," *Journal of Dentistry*, vol. 125, p. 104226, 2022, doi: 10.1016/j.jdent.2022.104226.
[10] L. Chen, M. S. Akram, A. Saleem, and H. Ullah, "Automatic street lighting system with vehicle detection using deep-learning based remote sensing," *International Journal of Engineering and Management Research*, vol. 12, no. 2, pp. 1–7, 2022, doi: 10.31033/ijemr.12.2.1.
[11] W. Zhao *et al.*, "Developing a new integrated advanced driver assistance system in a connected vehicle environment," *Expert Systems with Applications*, vol. 238, p. 121733, 2024, doi: 10.1016/j.eswa.2023.121733.
[12] J. Schleusner, H. Blume, and S. Lampe, "Dynamic model-based safety margins for high-density matrix headlight systems," *IEEE Transactions on Intelligent Transportation Systems*, vol. 24, no. 7, pp. 7296–7305, 2023, doi: 10.1109/TITS.2023.3264768.
[13] E. Vidal-Tortosa and R. Lovelace, "Road lighting and cycling: a review of the academic literature and policy guidelines," *Journal of Cycling and Micromobility Research*, vol. 2, p. 100008, 2024, doi: 10.1016/j.jcmr.2023.100008.
[14] T. N. Babu, T. Nakkeeran, V. Prasanna, and D. Rama Prabha, "Auto adjusting brightness of headlights using LDR and ultrasonic sensor to prevent night glare," *Turkish Journal of Computer and Mathematics Education*, vol. 12, no. 14, pp. 1020–1026, 2021.
[15] M. K. A. Kamarudin *et al.*, "Road traffic accident in Malaysia: trends, selected underlying, determinants and status intervention," *International Journal of Engineering & Technology*, vol. 7, no. 4.34, p. 112, 2018, doi: 10.14419/ijet.v7i4.34.23839.
[16] J. Sumithra, A. Sumalatha, A. Vanitha, B. Sivadharshini, V. S. Pandi, and S. Ravi, "A smart and systematic vehicle headlight operations controlling system based on light dependent resistor," in *Proceedings of the 2nd International Conference on Intelligent and Innovative Technologies in Computing, Electrical and Electronics, ICIITCEE 2024*, Bangalore, India, 2024, pp. 1–6. doi: 10.1109/IITCEE59897.2024.10467948.
[17] A. A. Raj, S. Giridharan, M. I. Ahammed, and P. Divya, "Adaptive vehicle headlight system using speed, indicator detection, and machine learning for real-time beam control," in *Proceedings of the International Conference on Intelligent Innovations in Engineering and Technology (ICIIET)*, Coimbatore, India, 2025, pp. 1–6.
[18] S. K. Okrah and O. S. W. E. F. Kumassah, "Design and implementation of automatic headlight dimmer for vehicles using light dependent resistor (ldr) sensor," *International Journal of Emerging Technology and Innovative Engineering*, vol. 2, no. 4, 2016, [Online]. Available: https://www.researchgate.net/publication/352261508
[19] H. Fechtner, M. Stenner, J. Schuster, T. Kliem, T. Teschner, and B. Schmuelling, "Automatic headlight leveling system with a modular design for the automotive aftermarket," in *IEEE International Conference on Consumer Electronics - Berlin, ICCE-Berlin*, 2019, pp. 357–362. doi: 10.1109/ICCE-Berlin47944.2019.8966139.
[20] F. Muhammad, D. D. Yanto, W. Martiningsih, V. Noverli, and R. Wiryadinata, "Design of automatic headlight system based on road contour and beam from other headlights," in *Proceeding - 2020 2nd International Conference on Industrial Electrical and Electronics, ICIEE 2020*, 2020, pp. 112–115. doi: 10.1109/ICIEE49813.2020.9276906.
[21] Z. Guan, H. Yang, and Z. Shi, "An optimized calculating method for the vehicle headlight automatic leveling system," in *Proceedings of the 2023 7th CAA International Conference on Vehicular Control and Intelligence, CVCI 2023*, 2023, pp. 1–4. doi: 10.1109/CVCI59596.2023.10397135.
[22] H. Zhang, Y. Shi, Z. Shi, C. Song, X. Yan, and B. Wu, "A headlight automatic leveling system with misadjustment suppression," in *2022 6th CAA International Conference on Vehicular Control and Intelligence, CVCI 2022*, 2022, pp. 1–5. doi: 10.1109/CVCI56766.2022.9965120.
[23] H. A. Harindu, J. R. Kithsiri, and C. Premachandra, "Improvement of driver visibility at night by ego vehicle headlight control," in *Proceedings of International Conference on Image Processing and Robotics, ICIPRoB*, 2020, doi: 10.1109/ICIP48927.2020.9367351.
[24] J. H. Connell, B. W. Herta, S. Pankanti, H. Hess, and S. Pliefke, "A fast and robust intelligent headlight controller for vehicles," in *IEEE Intelligent Vehicles Symposium, Proceedings*, 2011, pp. 703–708. doi: 10.1109/IVS.2011.5940492.
[25] R. Anjali, "A secured and automated vehicle surveillance system," in *Proceedings - 5th IEEE International Conference on Recent Trends in Electronics, Information and Communication Technology, RTEICT 2020*, 2020, pp. 127–130. doi: 10.1109/RTEICT49044.2020.9315591.
[26] S. Wang, X. Yang, Z. Chen, and Y. Zhang, "Integrated distributed model predictive control for vehicular platoon considering node vehicle dynamics," *IEEE Transactions on Vehicular Technology*, vol. 74, no. 8, pp. 11939–50, 2025, doi: 10.1109/TVT.2025.3554895.
[27] Y. Huang, W. Liang, and Y. Chen, "Stability regions of vehicle lateral dynamics: estimation and analysis," *Journal of Dynamic Systems, Measurement and Control, Transactions of the ASME*, vol. 143, no. 5, p. 51002, 2021, doi: 10.1115/1.4048932.
[28] D.-I. Matei, A. Negroiu, and G. Bucur, "Dc motor angular position control system using arduino platform," *Romanian Journal of Petroleum & Gas Technology*, vol. 5 (76), no. 2, pp. 105–118, 2024, doi: 10.51865/jpgt.2024.02.07.
[29] D. Chattejee, C. Chakraborty, and S. Dalapati, "Pulse-width modulation techniques in two-level voltage source inverters - state of the art and future perspectives," *Power Electronics and Drives*, vol. 8, no. 1, pp. 335–367, 2023, doi: 10.2478/pead-2023-0023.
[30] R. M. Jalnekar and K. S. Jog, "Pulse-width-modulation techniques: a review," *IETE Journal of Research*, vol. 46, no. 3, pp. 175–183, 2000.

[31] L. Zhang, M. Liu, Z. Sun, Y. Wu, and S. Zhou, "Requirements analysis and architecture design of automotive adaptive front-lighting system (AFS) based on functional safety standards," in *IEEE International Conference on Industrial Informatics (INDIN)*, Beijing, China, 2024, pp. 1–6, doi: 10.1109/INDIN58382.2024.10774379.

## BIOGRAPHIES OF AUTHORS

**Liew Hui Fang** is currently a senior lecturer at the Faculty of Electrical Engineering Technology at Universiti Malaysia Perlis. In 2012, she received her degree in Electrical Systems Engineering from University Malaysia Perlis (UniMAP), Malaysia. In 2015. M.Sc. degree in Microelectronics Engineering from University Malaysia Perlis (UniMAP), in 2018, she received the Ph.D. degree in Electrical Systems Engineering at University Malaysia Perlis (UniMAP). Her research interests include the analysis and development of new sources of energy harvesting systems and techniques, renewable energy, power energy, microwave communication, and RF MEMS. She can be contacted at email: hfliew@unimap.edu.my.

**Rosemizi bin Abd Rahim** was born in Kedah, Malaysia, in 1976. He received the B.Eng. degree in Electrical Engineering from Universiti Teknologi Mara, Malaysia, in 2000 and the M.Sc. degree in Electronic System Design Engineering from Universiti Sains Malaysia, in 2004. In 2013, he received a Ph.D. degree in Communication Engineering from Universiti Malaysia Perlis. From 2000 to 2004, he was a failure analysis engineer at a multinational electronic manufacturing company in Penang, Malaysia. His task was to resolve any failures that occurred during the production process of electronic products. Then, since 2005, he has been moved to Universiti Malaysia Perlis as an academician. His research interests include the analysis and development of new sources of energy harvesting systems and techniques, antenna design, and microwave engineering. Currently, he is a senior lecturer at the Faculty of Intelligent Computing at University Malaysia Perlis (UniMAP). He can be contacted at email: rosemizi@unimap.edu.my.

**Muhammad Izuan Fahmi Romli** obtained his Ph.D. degree and Master of Science from the University of Nottingham Malaysia Campus. In 2010, he received a Bachelor of Electrical Engineering Technology from Universiti Kuala Lumpur. Being active as an associate professor in the University Malaysia Perlis, his current interests lie in renewable energy, supercapacitors, optimization, and energy storage for electric vehicles. He can be contacted at email: izfahmi@gmail.com.

**A. A. M. Ezanuddin** currently serves as an assistant professor at Lincoln University College, Malaysia. He has also served as a Dean in the Faculty of Architecture and Engineering at LUCT, Cyberjaya, Malaysia (2021-2023), Spectrum College of Technology, Subang, Malaysia (2021), and previously at Lincoln University College (2019-2020). With over 10 years of experience in the education sector, he holds a PhD in Communication Engineering. Additionally, he has coordinated and spearheaded UniMAP's Institute of Electrical and Electronics Engineers student branch for several years. He has also worked as a field engineer maintaining communication, server workability, and ICT hardware at a state hospital. He can be contacted at email: ezanuddin@lincoln.edu.my.

**Shamshul Bahar Yaakob** received his bachelor's degree in Computer Engineering from Shizuoka University, Japan, and his Master of Engineering (M.Eng.) in Electrical and Electronic Systems from Nagaoka University of Technology, Japan. He is currently an Associate Professor at the Faculty of Electrical Engineering and Technology, Universiti Malaysia Perlis (UniMAP), Perlis, Malaysia. His research interests include soft computing, reliability optimization, and multi-criteria optimization, with applications in engineering system design and decision-making. He can be contacted at email: shamshul@unimap.edu.my.